AD-A086 333 NAVAL UNDERWATER SYSTEMS CENTER NEWPORT RI F/G 9/3
THE MAGNETIC CHARACTERISTICS OF TAPE WRAPPED CYLINDRICAL FERROM--ETC(U)
FEB 80 L J DALSASS
UNCLASSIFIED NUSC-TM-791227 NL

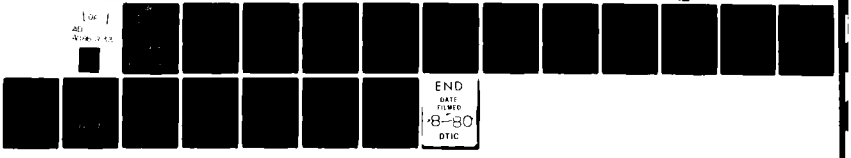

END
DATE FILMED
8-80
DTIC

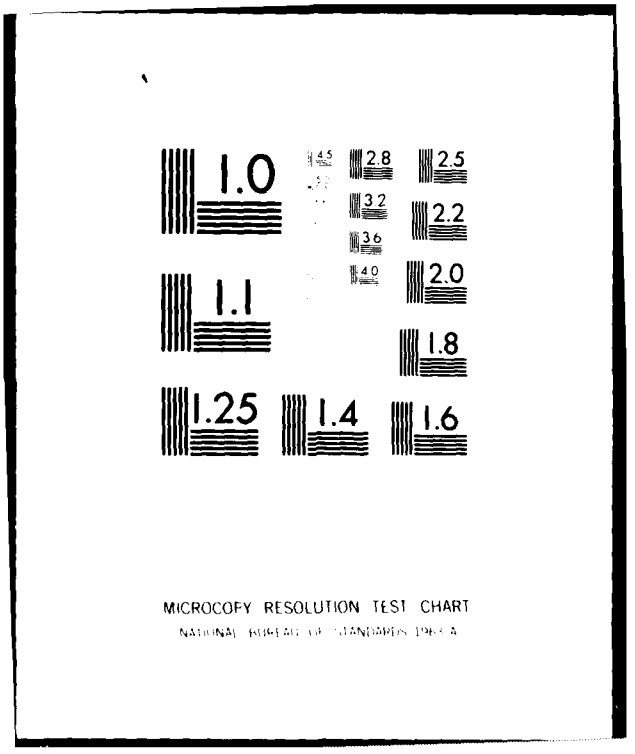
1.0
1.1
1.25
1.4
1.6
1.8
2.0
2.2
2.5
2.8
3.2
3.6
4.0
4.5
MICROCOPY RESOLUTION TEST CHART
NATIONAL BUREAU OF STANDARDS 1963-A

LEVEL II (14) DDC

NUSC-TM-791227

The Magnetic Characteristics of Tape Wrapped Cylindrical Ferromagnetic Laminations for Frequencies Below 50 KHz

(10) Louis J. Dalsass
Submarine Electromagnetic Systems Department

(12) 19

(11) 22 February 1980

DTIC ELECTE JUL 2 1980 S D

A

NUSC

NAVAL UNDERWATER SYSTEMS CENTER

Newport, Rhode Island • New London, Connecticut

406068 Gu 80 4 7 055

ABSTRACT

The leakage magnetic fields from magnetic devices are known to create EMI problems for sensitive shipboard VLF receivers and sonar equipment. Devices which contain ferromagnetic cores can be particularly significant EMI offenders because of the high flux densities available in their magnetic circuits.

This memorandum discusses the magnetic characteristics of various laminated cores found in shipboard equipment (with source frequencies extending into the VLF band). Test results are presented for an open tape cylindrical lamination containing an axial and radial air gap. Although this is a more complicated magnetic circuit, its behavior is shown to be identical to predictions derived for simple lamination shapes without air gaps for frequencies up to 50 kHz.

ADMINISTRATIVE INFORMATION

This memorandum was prepared under Project No. A51000, "Submarine R&D Electromagnetic Compatibility", Principal Investigator, D. S. Dixon, Code 344. The sponsoring organization is Naval Electronics Systems Command; Mr. J. Cauffman, Code 3041 is Program Manager; Technical Agent is Mr. H. DeMattia, Code 61R4 of the Naval Sea Systems Command.

TABLE OF CONTENTS

THE MAGNETIC CHARACTERISTICS OF TAPE WRAPPED CYLINDRICAL FERROMAGNETIC LAMINATIONS FOR FREQUENCIES BELOW 50 kHz

INTRODUCTION

High permeability ferromagnetic alloys are employed extensively in shipboard equipment. These alloys are used as magnetic cores in transformers, inductors and various signal conditioning and control devices. Unfortunately these devices generate magnetic fields that can couple with sensitive cables and circuits that are not adequately shielded or separated. This condition can degrade the performance of the susceptible system. The conditions that can cause the frequencies of the radiated emissions to extend into the operating bands of sonar and VLF receivers are:

1. operating a device in the non-linear region of its magnetic core B-H loop resulting in the generation of high order harmonics;

2. transient in-rush currents resulting from core switching effects;

3. line interruption/switching; and

4. powerline-conducted EMI.

Figure 1A is a simplified model of a typical magnetic device. The principal components are listed below.

C_1 = capacitance of the transmission line in farads
L_1 = inductance of the transmission line in henries
R_1 = resistance of the transmission line in ohms
R_2 = device resistance (includes dc resistance and contributions from eddy currents and hysteresis in ohms
L_p = device magnetizing inductance in henries
C_S = device shunt capacitance in farads

For highly inductive cores (large L_p), the circuit characteristics depend primarily on the frequency-dependent values of device resistance (R_2) and magnetizing inductance (L_p). If the applied frequency is less than the resonant frequency of the device, the shunt capacitance (C_S) may also be disregarded. The result of these approximations is the simplified circuit model shown in figure 1B.

EMC models of magnetic devices operating at sonar and VLF frequencies must account for variation of the circuit components (R_2) and L_p with frequency in those bands. The objective of this memorandum is to report test results for the magnetizing inductance (L_p) and permeability of an open tape wrapped cylindrical lamination.

DISCUSSION

COMMON LAMINATION GEOMETRIES

The magnetic core laminations in Navy equipment include a variety of shapes and sizes to accommodate particular applications. Figure 2 illustrates the following typical lamination categories which may be encountered.

- rectangular stampings
- toroidal geometries
- cylindrical cores

In figures 2A and 2B, the magnetic flux can be increased by grouping the laminations into thick stacks and adding a coil in the winding space of the laminations. A coil wrapped around the cylinder shown in figure 2C above the tape layers would, in some cases, create an air gap between the magnetic tape layer and coil.

SHIELDING THEORY

Mathematical expressions are available to determine the reduction in permeability with frequency for the idealized plane sheet and solid cylinder lamination cases shown in figures 3A and 3B[1]. A recent paper by Wait[2] discusses the toroidal cylinder. The assumptions made in most of these calculations is that the lamination boundaries are negligible (infinite length model) and the permeability does not depend on the amplitude of the exciting field (linear B-H loop).

PLANE SHEET SHIELDING

A plane sheet lamination with an initial permeability (μ_i) at a frequency of f = 0 Hz will have a lower permeability at higher frequencies due to the shielding effects of induced eddy currents that oppose the applied magnetic field. For the geometry of figure 3A and a simusoidal magnetic field applied as shown, the sheet permeability normalized to its initial value (μ/μ_i) is given in equation 1.

$$\frac{\mu}{\mu_i} = \frac{1}{\theta} \frac{\sinh \theta + \sin \theta}{\cosh \theta + \cos \theta} \tag{1}$$

In equation 2 below, the parameter (θ) is defined in terms of the frequency of the magnetic field (f), the electrical conductivity and initial magnetic permeability (μ_i) of the lamination (σ), and the lamination thickness (t).

$$\theta = 2\pi t \sqrt{\mu_i f \sigma} \tag{2}$$

A more convenient definition of θ is possible if it is expressed in terms of the ratio of lamination thickness (t) to skin depth thickness (δ). Because δ is defined by equation 3, θ can be rewritten as shown in equation 4.

$$\delta_i = \sqrt{\frac{1}{\pi f \mu_i \sigma}} \tag{3}$$

$$\theta = 2\pi^{1/2}\, t/\delta_i \tag{4}$$

The thickness, δ_i, is the distance in the lamination where the magnetic field is reduced to (1/e) of its surface value.

A more useful relationship for the ratio (μ/μ_i) is obtained if equation 1 is expanded in a power series for $\theta \ll 1$ and $\theta \gg 1$.

For $\theta \ll 1$

$$\frac{\mu}{\mu_i} = 1 - \frac{\theta^4}{30} + \frac{31\theta^8}{22{,}680} \cdots . \tag{5}$$

For $\theta \ll 1$, terms containing θ are insignificant relative to the constant term and can be dropped. The magnetic permeability can then be set equal to its initial value μ_i.

$$\lim_{\theta \to 0} \mu = \mu_i \tag{6}$$

For $\theta \gg 1$

$$\frac{\mu}{\mu_i} = \frac{1}{\theta}\left[1 - 2e^{-\theta}(\cos\theta - \sin\theta)\right]. \tag{7}$$

At VLF frequencies, the lamination thickness is often very many skin depths. For this case, the contribution made by the term containing $e^{-\theta}$ can be disregarded, reducing equation 7 to equation 8.

$$\lim_{\theta \gg 1} = \frac{\mu_i}{\theta} \tag{8}$$

Substituting θ from equation 2 into equation 8, we obtain:

$$\mu = \frac{1}{2\pi t}\sqrt{\frac{\mu_i}{f\sigma}} \tag{9}$$

Because t, μ_i, and σ are constants, the frequency dependence of μ from equation 9 is:

$$\mu \text{ proportional to } \frac{1}{\sqrt{f}} \tag{10}$$

SOLID CYLINDER SHIELDING

Similar results hold for a solid cylinder magnetic core.[1]

For $\theta \ll 1$

$$\frac{\mu}{\mu_i} = 1 - \frac{\theta^4}{48} + \frac{19\,\theta^8}{30,720} \tag{11}$$

$$\lim_{\theta \to 0} \mu = \mu_i \tag{12}$$

For $\theta \gg 1$

$$\frac{\mu}{\mu_i} = \sqrt{\frac{2}{\theta}}\left[1 + \frac{1}{4\sqrt{2}\,\theta} + \frac{1}{8\theta^2} \cdots\right] \tag{13}$$

$$\lim_{\theta \gg 1} \mu = \sqrt{\frac{2}{\theta}} \tag{14}$$

$$\text{or } \mu \text{ proportional to } \frac{1}{\sqrt{f}} \text{ as in equation 10.} \tag{15}$$

The permeability relations (equations 6, 10, 12, and 15) are characterized by:

- a constant permeability region ($\theta \ll 1$),
- a transition region, and
- a $1/\sqrt{f}$ dependence at high frequencies ($\theta \gg 1$).

TEST RESULTS

In figure 4, an open wrapped cylindrical lamination is shown that differs from the ideal lamination geometries discussed previously. This nonconformity results from the following factors, which are illustrated in the figure.

1. A transverse air gap exists between the lamination and magnetizing coil.
2. An axial air gap exists along the lamination which allows leakage flux to cross.
3. The lamination geometry is that of a hollow cylinder with a thin wall thickness relative to the cylinder diameter.

An inductor containing the cylindrical lamination was constructed as shown in figure 4 to determine its magnetic characteristics at frequencies up to 50 kHz. An important feature of this work was to determine any departures from the behavior of the ideal laminations previously discussed. A Hewlett Packard 4800A impedance meter was used to measure $|Z|$ and θ, (the impedance magnitude and phase) for frequencies up to 50 kHz. Test results are shown in figure 5.

At frequencies less than 50 kHz, the shunt capacitance and lead impedance of the test inductor are not significant, which results in the simplified circuit model shown in figure 1B. The input impedance of this network can be written as:

$$\vec{Z}(f) = R_2(f) + j\omega L_p(f) \tag{16}$$

where:

$\vec{Z}(f)$ = frequency dependent complex impedance in ohms
ω = angular frequency in radians per second
$j = \sqrt{-1}$.

From equation 16:

$$\omega L_p = |Z| \sin \theta \tag{17}$$

and

$$R_2 = |Z| \cos \theta \ . \tag{18}$$

Solving equation 17 for L_p yields equation 19:

$$L_p = \frac{1}{\omega} |Z| \sin \theta \ . \tag{19}$$

A program was written on the HP 25C calculator to compute values of L_p from the measured values $|Z|$ and θ. The program steps are listed in table 1. Note that R_2 is also available in storage register number 4.

Figure 6 shows the measured inductance in millihenries obtained from equation 19 over the frequency range from 100 Hz to 50 kHz. In figure 7, the inductance at each frequency shown in figure 6 was divided by the inductance at 100 Hz, converted to decibels, and plotted starting at 1 kHz. This procedure permits changes relative to the low frequency inductance to become more apparent.

The frequency corresponding to the start of the high eddy current band can be determined by superimposing an $f^{-1/2}$ line (10 dB per decade fall off) on the results of figure 7. Between 10 kHz and 50 kHz, the 10 dB/decade line is in excellent agreement with the slope of the normalized inductance curve; below 10 kHz, it begins to depart from the measured results. Therefore, the start of the high eddy current band was determined to be 10 kHz.

In summary, the test inductor with an open wrapped cylindrical lamination of HYM μ800, 0.014 inches thick, can be categorized as follows.

- for $f \leq 600$ Hz; the inductance is constant
- for 600 Hz $< f <$ 10 kHz - transition band
- for $f \geq 10$ kHz; the inductance varies as $f^{-1/2}$

From the plots shown in figures 6 and 7, we can conclude that the results for the test inductor are consistent with the frequency dependence expected for ideal laminations.

LAMINATION MAGNETIC PERMEABILITY

The magnetic permeability of the lamination used in the test inductor of figure 4 can be determined from direct measurements of coil inductance (figure 6), the crossectional areas of the lamination and solenoid, and the lamination pitch. Reference 3 provides details of the calculation. Application of these factors to the data in figure 6 is shown in figure 8. The magnetic permeability that corresponds to the constant inductance region (μ_i) of figure 6 is 1208 μ_o, where μ_o is the free space value of $4\pi \times 10^{-7}$ henries/meter. The reduction in permeability over the frequency band from 100 Hz to 50 kHz shown in figure 8 will have the same frequency variation as the inductance (figure 6), because the conversion factors relating both are independent of frequency.

Using a frequency of 10 kHz, which was determined earlier as the start of the high eddy current band, the measured electrical conductivity of the lamination (σ), and the magnetic permeability (μ_i), we can calculate the skin depth (δ_i) at the band edge (10 kHz). Therefore, using the definition of δ_i in equation 3:

$$\delta_i = \sqrt{\frac{1}{\pi f \mu_i \sigma}} \tag{20}$$

and inserting the following values,

$f = 10$ kHz
$\sigma = 5.07 \times 10^5$ siemens
$\mu_i = 1208\ \mu_o$,

we obtain

$$\delta_i = 2.03 \times 10^{-4} \text{ meters.}$$

Using the lamination thickness (t) in the test inductor of 0.014 inch (3.56×10^{-4} meters), the ratio t/δ_i at 10 kHz becomes:

$$\frac{t}{\delta_i} = \frac{3.56 \times 10^{-4} \text{m}}{2.03 \times 10^{-4} \text{m}} = 1.75 \tag{21}$$

An approximate θ value corresponding to the band edge at 10 kHz can be obtained by substituting t/δ_i into equation 4, resulting in:

$$\theta = 2\pi^{\frac{1}{2}} \left(\frac{t}{\delta_i}\right) = 6.2 \ . \qquad (22)$$

This θ value provides a quantitative limit for the expression $\theta >> 1$, in the case of an open cylindrical lamination.

CONCLUSION

From an EMC viewpoint, modeling of the magnetic characteristics of a tape wound cylindrical lamination containing radial and axial air gaps can be predicted from ideal shielding theory for $\theta >> 1$. The frequency marking the start of the high eddy current band (shown in figure 6) occurs when the lamination thickness is equal to 1.75 skin depths.

The circuit behavior of a test inductor using the cylindrical lamination as a magnetic core was found to be equivalent to a series-connected RL network (figure 1B) for frequencies from 100 Hz to 50 kHz. The components R and L, however, are dependent on the frequency of the applied magnetic field generated within the interior of the test inductor. This behavior results in a device impedance which is more complex than would be expected for constant RL components as observed in the test results of figure 5.

A program written for the HP 25C calculator was used to obtain the inductance (L) and lamination magnetic permeability (μ) of the test inductor in the band from 100 to 50 kHz. A step in the program was reserved, (Step 5 - Table 1) to permit the equivalent core loss resistance to also be determined.

REFERENCES

1. Bozorth, R. M., Ferromagnetism, D. Van Nostrand, chap. 17. 1951.

2. Wait, J. R., "The Electromagnetic Basis for Nondestructive Testing of Cylindrical Conductors", IEEE Transactions on Instrumentation and Measurement, Vol. IM-27, No. 3, September 1978.

3. Cafaro, A. D., "A System to Measure Longitudinal Variations of Magnetic Permeability in Ferromagnetic Strips," NUSC Technical Memorandum No. EA33-300-75, 15 December 1975.

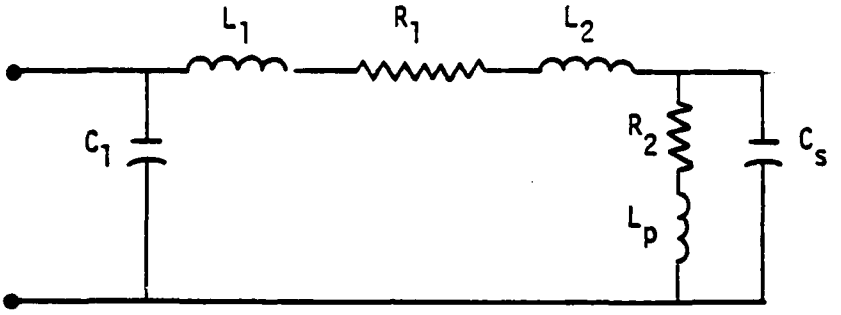

Figure 1A. Circuit Model of a Magnetic Device

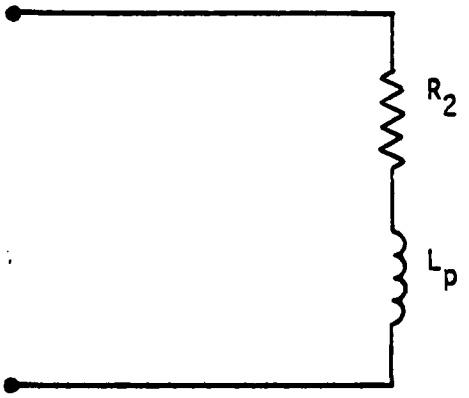

Figure 1B. Simplified Circuit Model

Figure 1. Magnetic Device Circuit Models

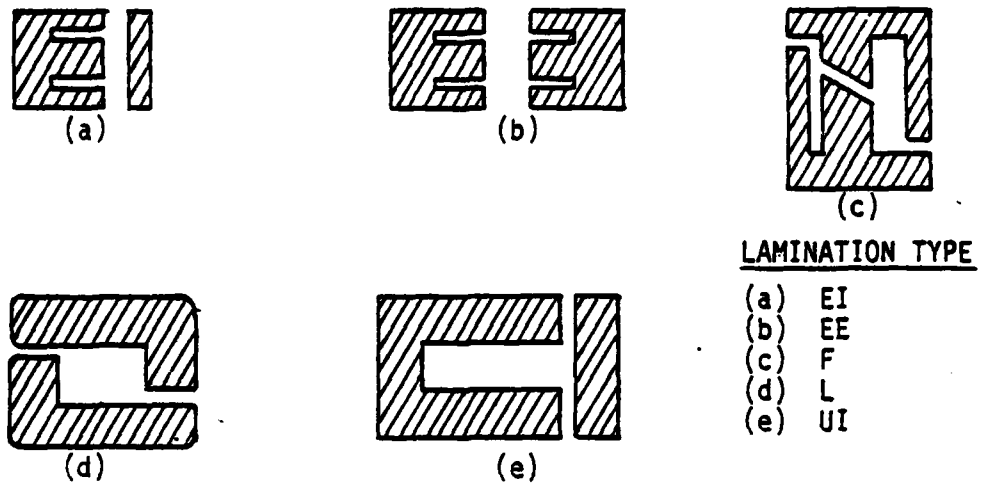

Figure 2A. Rectangular Laminations

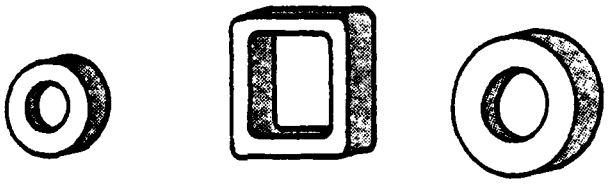

Figure 2B. Toroidal Laminations

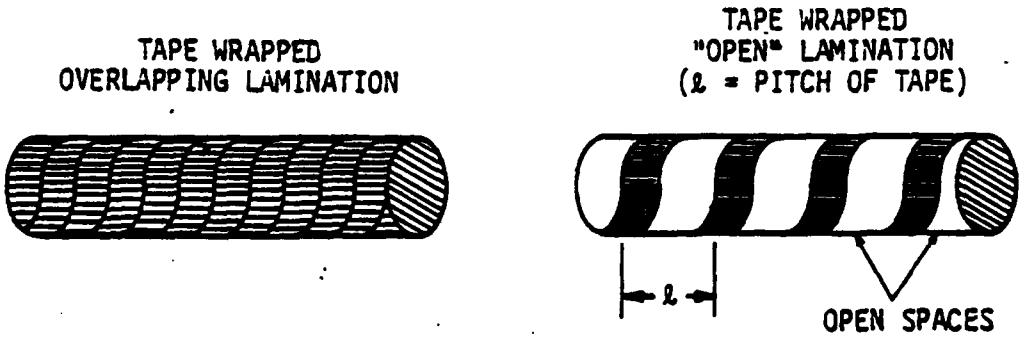

Figure 2C. Cylindrical Tape Wound Laminations

Figure 2. Typical Magnetic Lamination Shapes

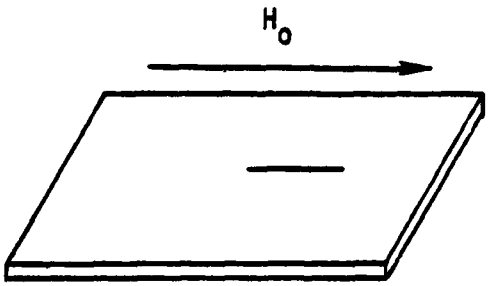

Figure 3A. Plane Sheet Shielding

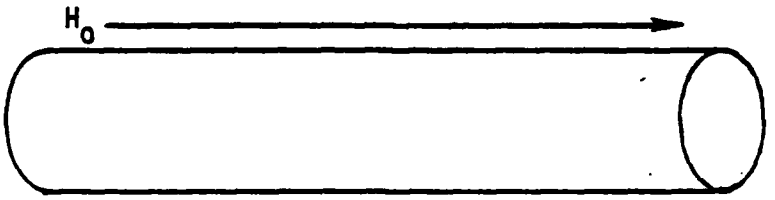

Figure 3B. Solid Cylinder

Figure 3. Shielding Theory Models

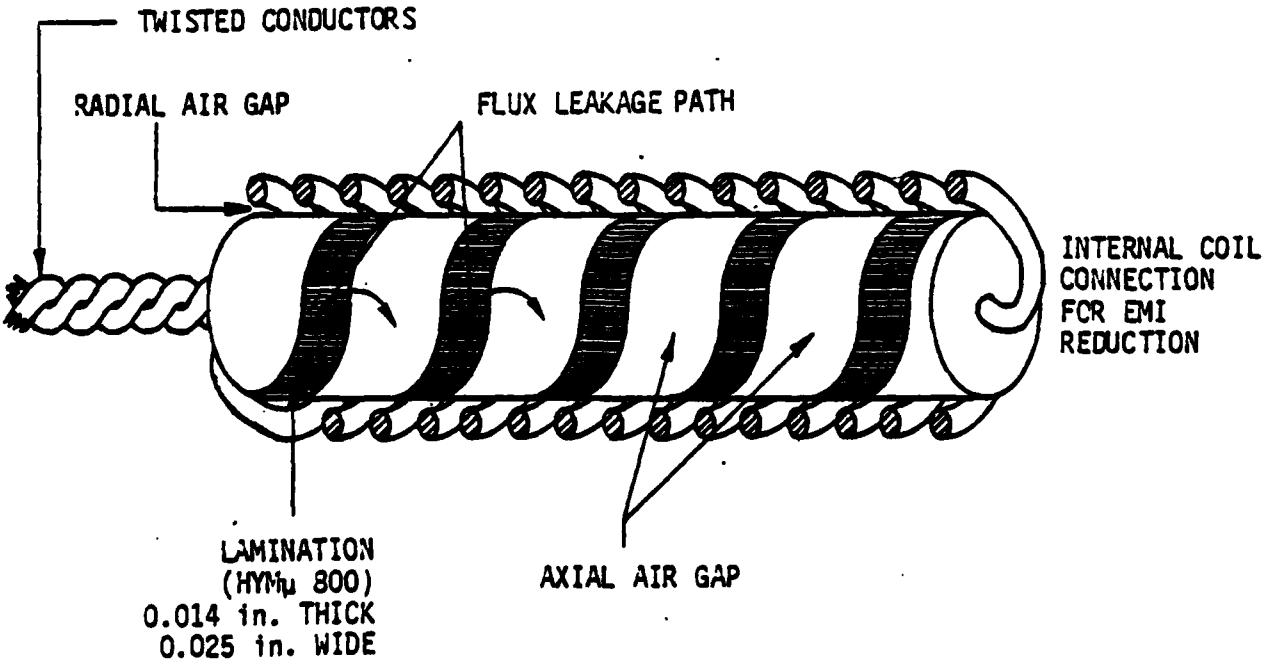

Figure 4. Tape Wound Open Cylindrical Lamination

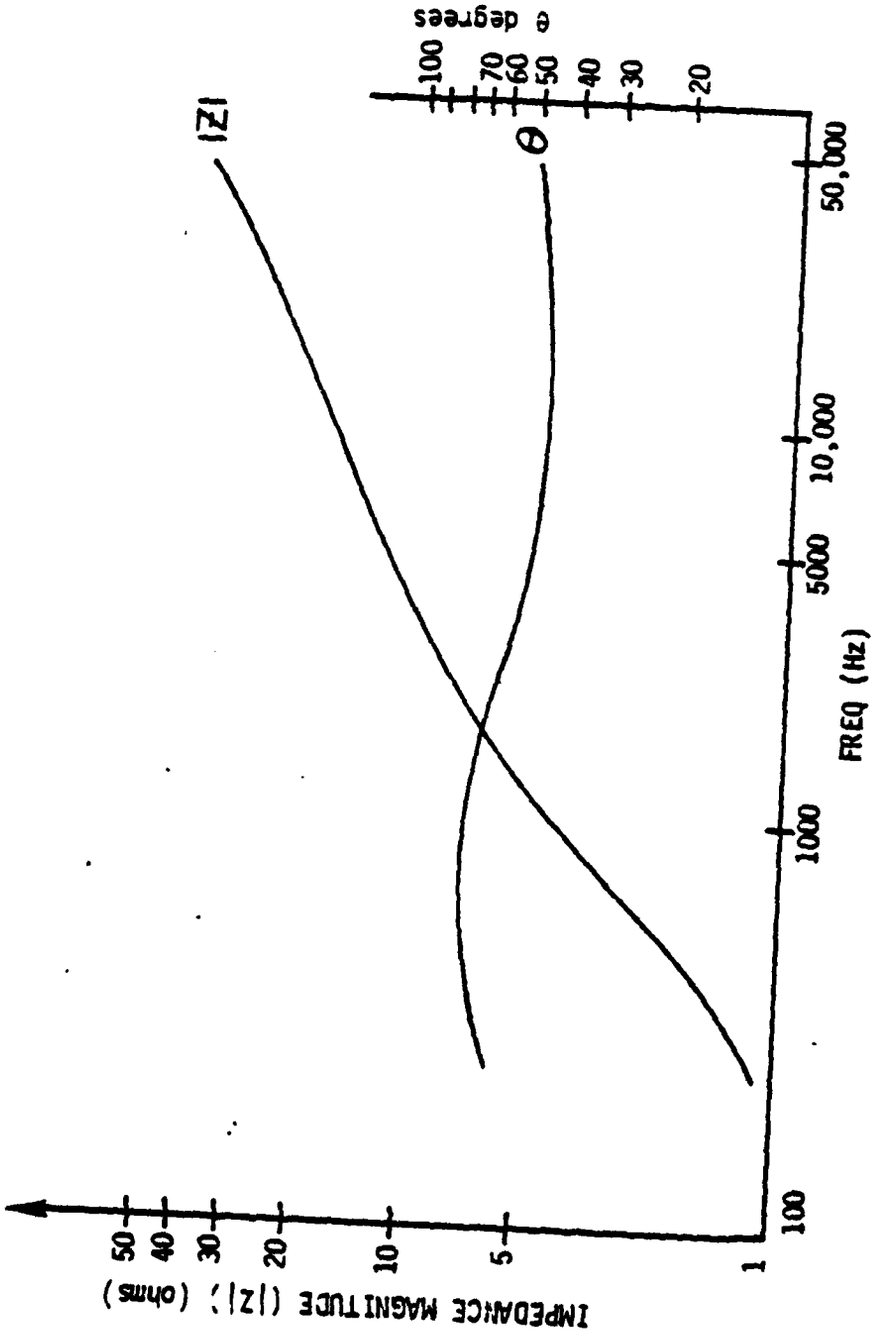

Figure 5. Magnitude and Phase of Impedance of Test Sample from 100 to 50,000 Hz

Table 1. HP 25C Program Steps to Calculate the Frequency Dependence of the Test Sample Inductance (L_p and Resistance (R_2)

A. INITIAL ENTRIES

STORE IN REGISTERS NUMBER:

1. Angular frequency ($2\pi f$)
2. Impedance magnitude $|Z|$
3. Phase Angle (θ)

B. STEP NUMBER

1. Recall (Contents of) Register 3
2. Cosθ
3. Recall Register 2
4. X (Multiply)
5. Store (Results of Step 4) in Register 4 (R_2)
6. Recall Register 3
7. Sinθ
8. Recall Register 2
9. X
10. Recall Register 1
11. (Divide)
12. Store Register 5 (L_p)

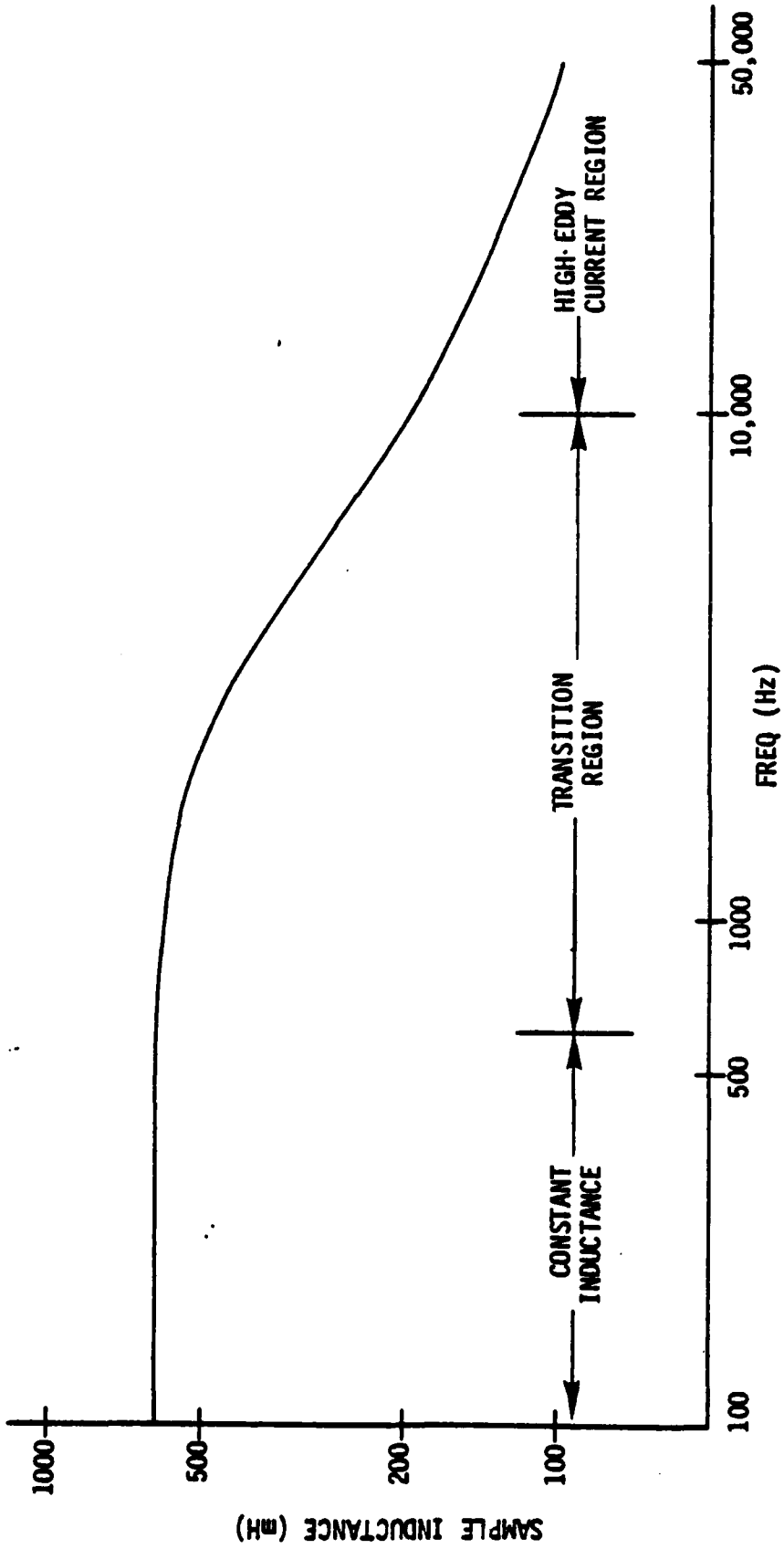

Figure 6. Test Sample Inductance in Millihenries vs Frequency from 100 to 50,000 Hz

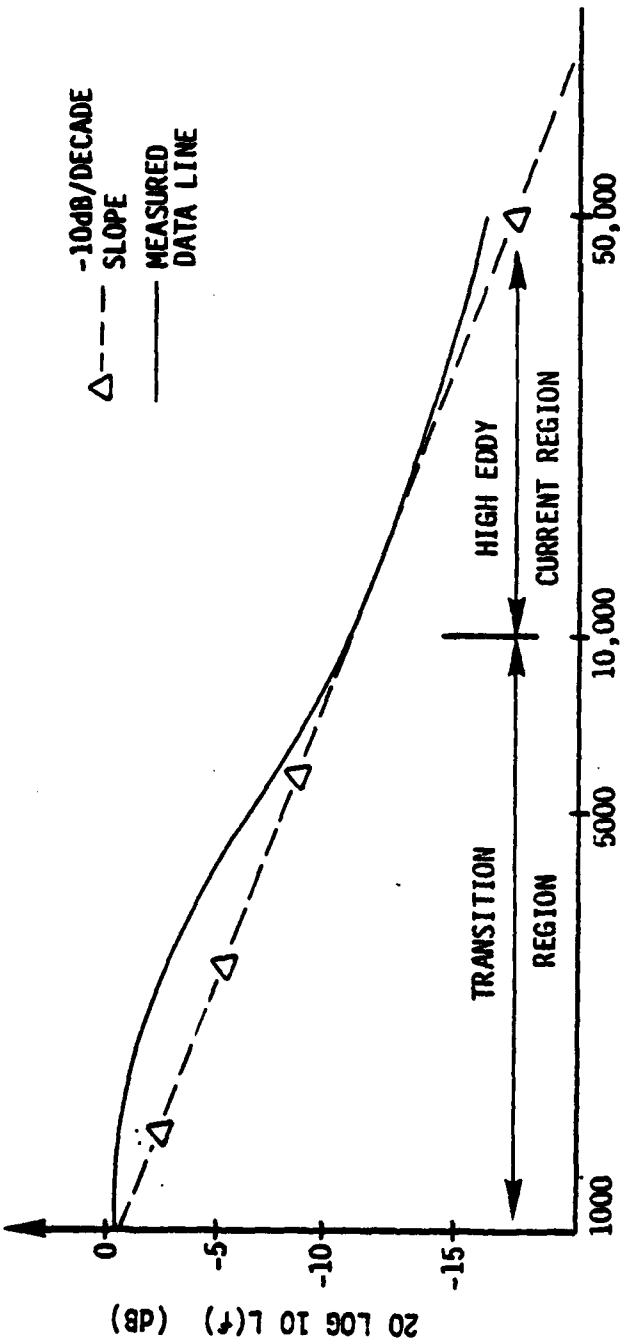

Figure 7. Test Sample Inductance after Normalizing to the Zero Frequency (dc) Inductance in Decibels for Frequency Range from 1000 to 50,000 Hz

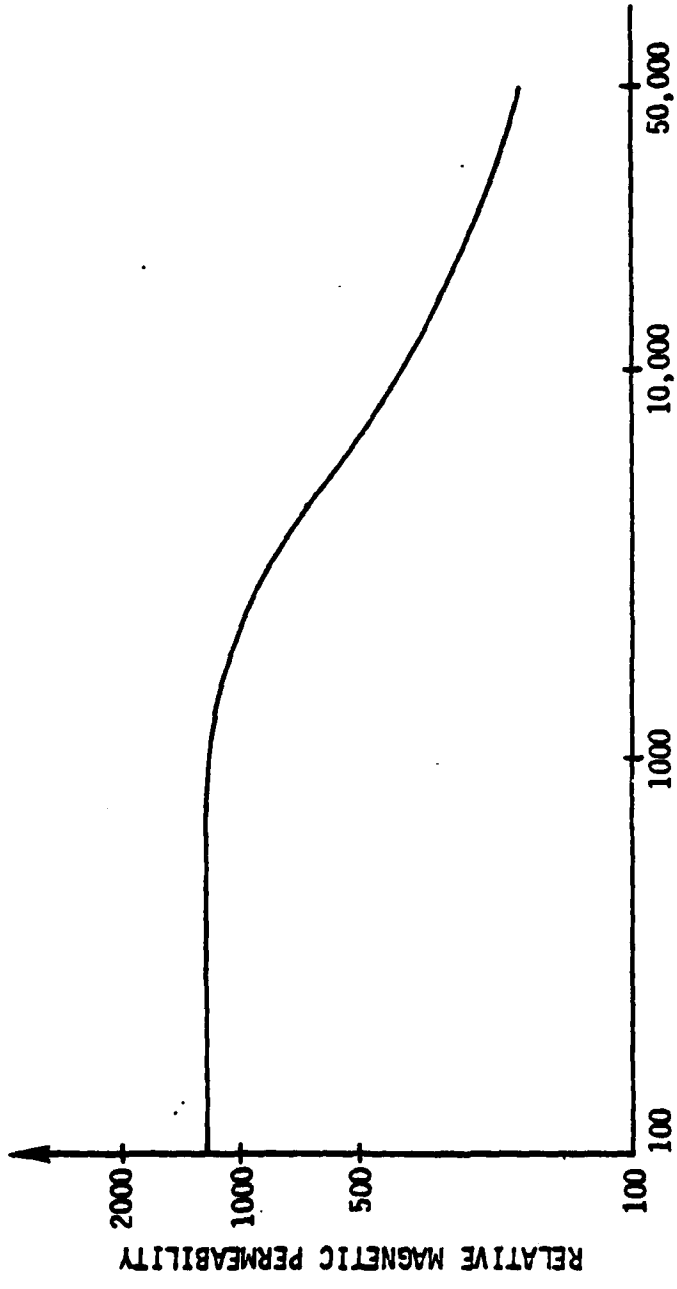

Figure 8. Lamination Permeability in the Frequency Band from 100 to 50,000 Hz

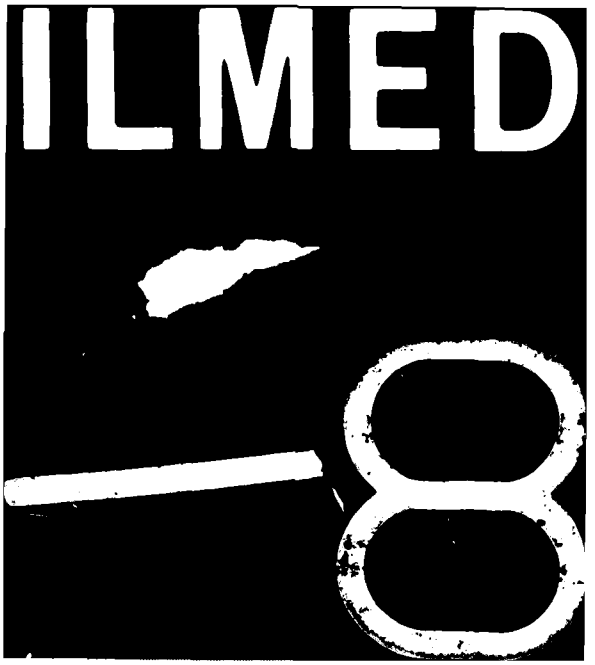
ILMED